

1-1-2021

The multidisciplinary approaches on facies developments and depositional systems of the Bahçecik travertines, Gümüşhane, NE-Turkey

RAİF KANDEMİR

EZHER TAGLIASACCHİ

MİNE SEZGÜL KAYSERİ ÖZER

DİLEK ŞAFFAK

FATİH KÖROĞLU

See next page for additional authors

Follow this and additional works at: <https://journals.tubitak.gov.tr/earth>

 Part of the [Earth Sciences Commons](#)

Recommended Citation

KANDEMİR, RAİF; TAGLIASACCHİ, EZHER; ÖZER, MİNE SEZGÜL KAYSERİ; ŞAFFAK, DİLEK; KÖROĞLU, FATİH; HU, HSUN-MING; and SHEN, CHUAN-CHOU (2021) "The multidisciplinary approaches on facies developments and depositional systems of the Bahçecik travertines, Gümüşhane, NE-Turkey," *Turkish Journal of Earth Sciences*: Vol. 30: No. 5, Article 1. <https://doi.org/10.3906/yer-2104-20>
Available at: <https://journals.tubitak.gov.tr/earth/vol30/iss5/1>







This Article is brought to you for free and open access by TÜBİTAK Academic Journals. It has been accepted for inclusion in Turkish Journal of Earth Sciences by an authorized editor of TÜBİTAK Academic Journals. For more information, please contact academic.publications@tubitak.gov.tr.

The multidisciplinary approaches on facies developments and depositional systems of the Bahçecik travertines, Gümüşhane, NE-Turkey

Authors

RAİF KANDEMİR, EZHER TAGLIASACCHİ, MİNE SEZGÜL KAYSERİ ÖZER, DİLEK ŞAFFAK, FATİH KÖROĞLU, HSUN-MING HU, and CHUAN-CHOU SHEN

The multidisciplinary approaches on facies developments and depositional systems of the Bahçecik travertines, Gümüşhane, NE-Turkey

Raif KANDEMİR^{1*} , Ezher TAGLIASACCHI² , Mine Sezgül KAYSERİ ÖZER³ , Dilek ŞAFFAK¹, Fatih KÖROĞLU⁴ , Hsun-Ming HU^{5,6} , Chuan-Chou SHEN^{5,6} 

¹ Department of Geological Engineering, Faculty of Engineering and Architecture, Recep Tayyip Erdoğan University, Rize, Turkey

² Department of Geological Engineering, Faculty of Engineering, Pamukkale University, Denizli, Turkey

³ Dokuz Eylül University, Institute of Marine Science and Technology, İzmir, Turkey

⁴ Department of Geological Engineering, Faculty of Engineering and Graduate School of Natural and Applied Sciences, Ankara University, Ankara, Turkey

⁵ High-Precision Mass Spectrometry and Environment Change Laboratory (HISPEC), Department of Geosciences, National Taiwan University, Taipei, Taiwan, ROC

⁶ Research Center for Future Earth, National Taiwan University, Taipei, Taiwan, ROC

Received: 23.04.2021

Accepted/Published Online: 04.08.2021

Final Version: 28.09.2021

Abstract: The Bahçecik travertines, located in Gümüşhane (NE-Turkey) have been investigated for the first time using a multidisciplinary approach, which included sedimentological (lithofacies, depositional system), petrographic, radiometric ²³⁰Th dating, geochemical analysis (stable isotopes), palynomorphs and geophysics (GPR). A carbonate build-up, 12 m thick, was formed with some interruptions, through the middle Pleistocene period. For this study, two travertine sections (F and D) were extensively used to figure out palaeoenvironmental and palaeoclimatic proxies. The main precipitation cycles, separated by palaeosol levels, have been described and interpreted from a sedimentological perspective. The carbonate deposits consist of shrubs, crystalline crust, reed, laminated (micritic), pisoids, oncoids, calcite thin rafts and coated gas bubbles, lithoclasts, and palaeosol levels. The sedimentological fieldwork and petrographic analysis show that the Bahçecik travertines formed in depression depositional and slope depositional systems. Moreover, the first ²³⁰Th ages, stable isotopic results and palynofloral data in this study, prove that the Bahçecik travertines might have been affected by climatic and tectonic interruptions. According to dating results, the travertine occurrences began to precipitate during the 353 ka and continued into the 263 ka. Based on the palynological data, an abundance of herbaceous plants species was recorded in the warming period of climate. The thickness ranges from 2 to 12 m of the Bahçecik travertines. This precise thickness and also the presence of two different travertine formations, separated by a palaeosol erosional surface, were recorded by the ground penetrating radar (GPR) geophysical method.

Key words: Travertine, depositional system, radiometric dating, stable isotopes, middle Pleistocene, Gümüşhane

1. Introduction

Travertine, tufa and speleothem represent all the terrestrial carbonate precipitation deposited around the rivers, springs, lakes, and caves when CO₂-rich, Ca-bearing waters are subjected to mainly low pressure at surface conditions (Guo and Riding, 1998; Fouke et al., 2000). These carbonate occurrences are a remarkable archive of the hydrological, tectonic, environmental, and climatological conditions of the period when they formed (Andrews et al., 1997; Hancock et al., 1999; Minissale et al., 2002; Pedley, 2009; De Filippis et al., 2012; Özkul et al., 2013; Gandin and Capezzuoli, 2014). Until now, these terrestrial carbonates were preferred for palaeoenvironmental and palaeoclimatic reconstructions because stable isotopes in travertines are less predictable in terms of disequilibrium effects (Andrews, 2006; Arenas et al., 2007, 2010; Bertini et al., 2014; Toker et al., 2015; Tagliasacchi and Kayseri-Özer, 2020). Global climate changes can also influence the depositional architecture and the geochemical features of travertines (Mancini et al., 2019; Rickets et al., 2019).

Travertines are chemically-precipitated continental limestones, whose precipitation is mainly due to carbon dioxide degassing from a groundwater source leading to calcium carbonate supersaturation (Pentecost, 2005). Based on the origin of the CO₂ interacting with the groundwater, Pentecost (2005) classified terrestrial carbonates into two groups: thermogene and meteogene types. Thermogene travertine, of massive texture, which is generally laminated, less porous and low in organic material content, is deposited from relatively hot water thermal springs. Meteogene travertine, which corresponds to the tufa term, is usually soft, generally highly porous and containing higher plant and animal remains, is formed from relatively cold water springs (Guo and Riding, 1998; Pentecost, 2005).

In this study, tufa and speleothem deposits are not included because the investigated area is mainly composed of travertine precipitation. The palaeoenvironmental and palaeoclimatic implications of travertines, located in the Gümüşhane and Bayburt regions, have remained an unknown. Hence the Eastern Pontides (eastern Sakarya Zone) still preserved some mystery surrounding terrestrial

*Correspondence: raif.kandemir@erdogan.edu.tr

carbonate occurrences. Studies have mainly focused on their geotechnical properties as decoration stone but the limited geological, geochemistry and formation conditions of the Gümüşhane and Bayburt region's travertines and onyx marbles. Yalçınalp et al. (2008) imply that there are important travertine deposits in the eastern Black Sea Region, especially in Bayburt, Gümüşhane, and Şiran areas. Yalçınalp et al. (2008) also suggest that the physicochemical properties and formation condition of Bahçecik travertines as the biggest travertine deposit in the Gümüşhane region, were determined by its morphological properties and formation conditions, and the reserve of the Bahçecik travertines are about 400.000 m³. Arslan et al. (2005) stated that petrological and limited geochemistry resulted in the travertines in the Gümüşhane and Bayburt regions. They suggested that Bahçecik travertines have typical meteogene (low-temperature) characteristics and the extent of deposits is entirely related to main tectonic lines and basement carbonate rocks (Berdiga Formation).

Travertine quarries provide good opportunities to investigate in detail but they are very restricted. Recently, ground penetrating radar (GPR) development has become very effective and the most powerful noninvasive geophysical prospecting method that can image shallow subsurface features (Öğretmen and Şeren, 2014). It can also be used to identify the detailed subsurface geometry and characteristics of travertines (e.g., Silva et al. 2004; Porsani et al., 2006; Kadioğlu, 2008; Yalçiner, 2013; Öğretmen and Şeren, 2014). Yalçiner (2013) described the subsurface geometry of fissure-ridge travertine in Pamukkale (Denizli, SW-Turkey) by using the GPR geophysical method.

The present study aims to explain the travertine facies and depositional systems, geochemistry, stable isotopic records, palynology, and ²³⁰Th age results and GPR determinations (100 MHz radargram profiles) of the travertine deposits located in the Bahçecik region at Gümüşhane (NE-Turkey). Sedimentological, petrographic and palynological investigations of the Quaternary travertines were carried out for the first time in this study using the multidisciplinary approach of the eastern part of the Sakarya Zone. It is aimed to make an important contribution to the literature by comparing the information obtained from the Bahçecik travertines with other similar travertine locations.

2. Geological setting

The study area is located at the northeast of Bahçecik, 12 km to the west of the Gümüşhane settlement in the eastern part of the Sakarya Zone, NE Turkey (Figure 1a). There is a heterogeneous pre-Jurassic basement in the eastern part of the Sakarya Zone. It contains Upper Paleozoic units, composed of metamorphic rocks of ~323 Ma age (lower Pennsylvanian) (Topuz et al., 2007) and granites of ~302 Ma age (upper Pennsylvanian) (Karsli et al., 2016; Dokuz et al., 2017), and Permo-Carboniferous shallow marine to terrigenous sedimentary rocks (Okay and Leven, 1996; Çapkınoğlu 2003). These heterogeneous basement rocks are unconformably overlain by the Lower to Middle Jurassic aged Şenköy Formation. The Şenköy Formation is characterized by a volcano-sedimentary unit consisting of andesite, basalt, and their pyroclastics intercalated with conglomerates, sandstones

and Ammonitico Rosso type sediments (Kandemir, 2004). The Şenköy Formation is conformably overlain by the Upper Jurassic-Lower Cretaceous aged Berdiga Formation, which is made up of platform-type carbonates (Pelin, 1977). The lower part of this formation starts with grey-white and beige-colored thick-massive bedded dolomite and dolomitic limestones. The upper part of the formation is characterized by grey-white colored limestones (Özyurt et al., 2019). The Berdiga Formation is the oldest unit in the Bahçecik area (Figure 1b). The Berdiga Formation is conformably overlain by the Upper Cretaceous aged Kermutdere Formation (Tokel, 1972). The formation essentially consists of turbiditic sequences (Yılmaz and Kandemir, 2006). The basal part of the formation is made up of yellowish-colored calcarenites and red-colored micritic limestones rich in planktonic microfauna (Globotruncanidea). This unit passes upward into the siliciclastic turbidite facies locally with interbedded felsic tuffs (Okay and Şahintürk, 1997; Yılmaz et al., 2008). These units are unconformably overlain by the Eocene Kabaköy Formation, which is composed of andesite, basalt, and their pyroclastics interbedded with sedimentary rocks (Güven, 1993). The region was affected by vertical faults oriented NE-SW, leading to the travertine formation (Figure 1b). Travertines unconformably cover all these units. The average thickness of travertines was determined as 12–14 m by the GPR applications (Şaffak, 2018).

3. Materials and methods

Several analyses followed the multiproxy approaches to reconstruct travertine occurrences after detailing sedimentary logs obtained from the investigated site. This study focuses on two main sections (F and D sections, Figure 1b). Two sedimentary logs, (12 and 4 m, respectively) were taken from the Bahçecik site (Figures 2b–2d). Lithotype interpretations of travertines have been done based on describing terrestrial carbonates of Guo and Riding (1998), Arenas-Abad et al. (2010), and Capezzuoli et al. (2014). In total, 60 compact carbonate and palaeosol samples were systematically obtained from these sections for the laboratory part. The laboratory analyses (²³⁰Th dating, stable isotopes, and palynology) were performed in collected samples. ²³⁰Th dating on six travertine samples was determined at the High-Precision Mass Spectrometry and Environment Change Laboratory (HISPEC) of the National Taiwan University (Shen et al., 2012; Cheng et al., 2013). The stable carbon and oxygen isotope measurements of 54 Bahçecik travertine samples were analyzed at the carbonate laboratory of stable isotopes, Department of Geoscience, University of Arizona (USA). A total of 95 carbonate samples systematically obtained from the F and D sedimentary logs were analyzed in thin sections for description and interpretation of petrographic analysis. The 24 core carbonate and 4 palaeosol samples were compiled for palynological analysis. Selected fine-grained palaeosol samples of 5–10, were processed using the standard palynological preparation methods of HCl, HF, and acetolysis treatments. Sample preparation and point counting were performed at the palynological laboratory of the Direnç Mühendislik (Ankara, Turkey) and the Institute of Marine Science and Technology of Dokuz Eylül University in İzmir, Turkey.

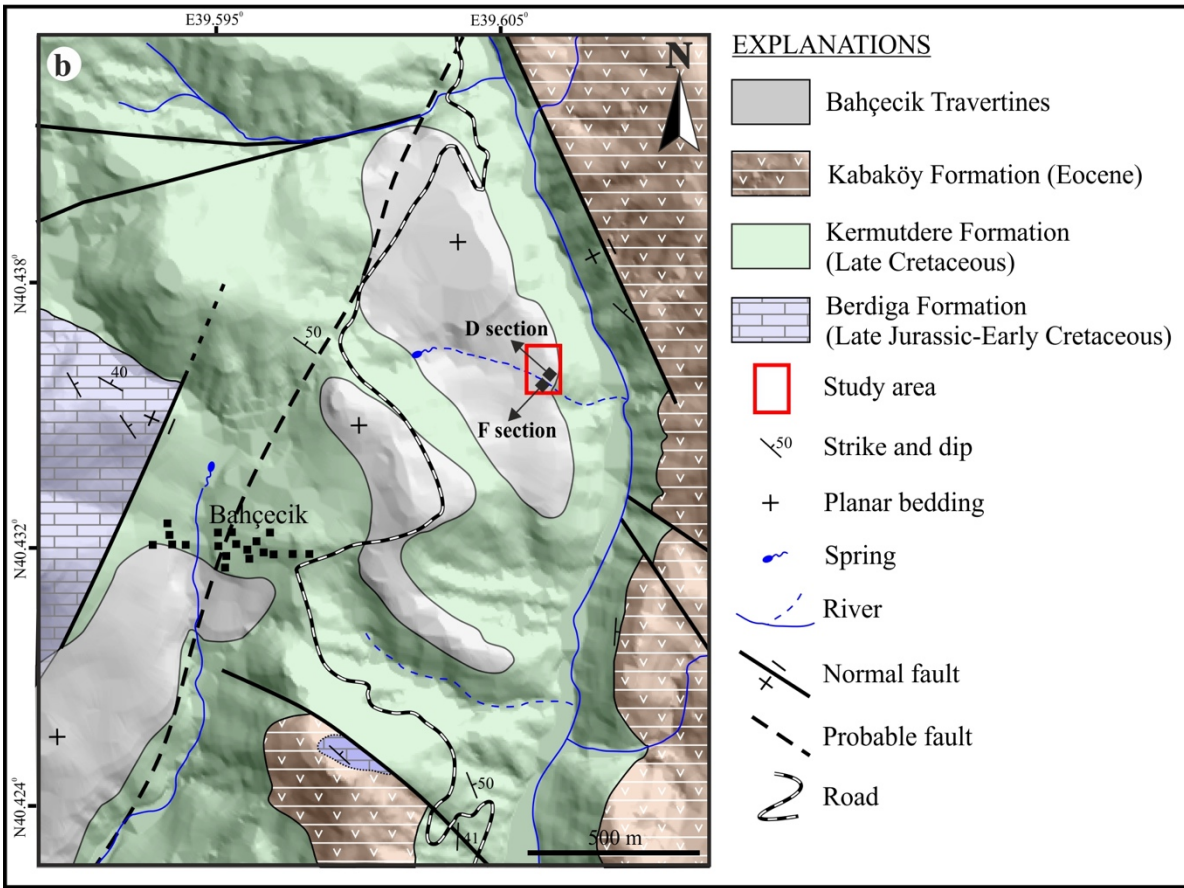
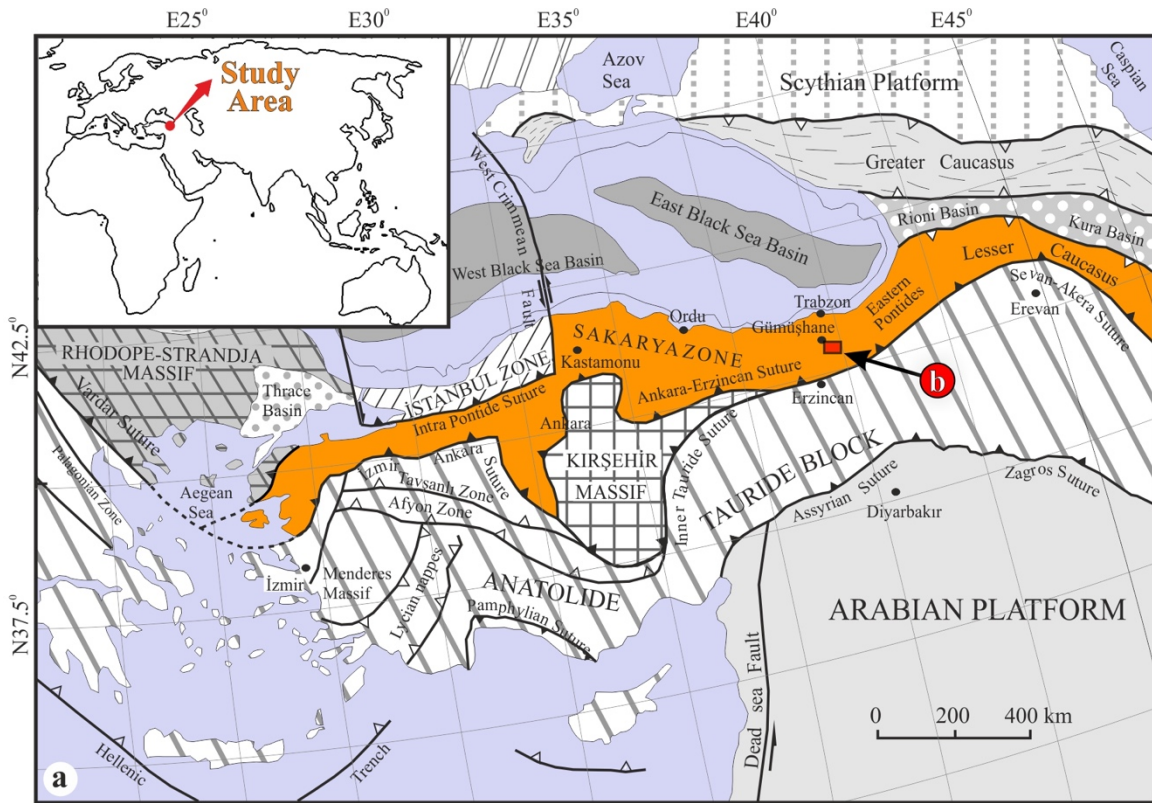


Figure 1. (a) Regional tectonic map of Turkey showing the main continental blocks, structure zones, and plate boundaries (modified from Okan and Tüysüz, 1999); (b) simplified geological map of the Bahçecik travertine areas and surroundings, Gümüşhane, NE-Turkey.



Figure 2. (a) Panoramic view of the Bahçecik travertine deposition; (b) Horizontal laminated (micritic) travertine sequence intercalated with the palaeosol level, which deposited in a depression depositional system (shrub flat; flat-pool facies); (c) Slope depositional system characterized by smooth slope and terrace slope facies (terrace pool and terrace rim subfacies); (d) Closer view of terrace slope facies with significant karstic cavities; (e and f) crystalline crust and micritic laminae formed in terrace rim and terrace pool subfacies; (g) Closer view of “f” that illustrates lithoclasts, coated gas bubbles and shrubs in slope depositional system (smooth slope facies); (h) Gastropod shells observed in palaeosol level; (i) Macro sample of reed lithotype (scale is 12 cm).

In this study, ground penetrating radar (GPR) was applied to these fields in order to identify sedimentary features, travertine continuity, and thickness of travertines. GPR data were acquired using a 100 MHz unshielded antenna on profiles. Generally, radargrams obtained from GPR profiles displayed different stratigraphical and main palaeosol levels (Şaffak, 2018). GPR uses a high-frequency radio signal transmitted into the ground, and reflected signals were returned to the receiver and stored on digital media (Conyers, 2006). The computer measures the time taken for a pulse to travel to and from the target, indicating their depth and location. Continuous cross-sectional profiles were produced by using the GPR method in the investigated area.

4. Results

4.1. Lithofacies of the Bahçecik travertines

In the present study, depending on fieldwork and microscopic studies, lithofacies descriptions and interpretations of the Bahçecik travertines and detrital clastics associated with carbonate occurrences have been determined. The Bahçecik travertine deposits are composed of 8 distinguished travertine lithofacies that correspond to lithotypes and palaeosol level (Figure 2b). These are; a) shrubs, b) crystalline crust, c) reed, d) laminated (micritic), e) pisoids, f) oncoids, g) calcite thin rafts and coated gas bubbles, h) lithoclasts, and palaeosol, respectively. A description and interpretation of all lithofacies and their depositional systems of the Bahçecik travertine occurrences are given below in detail.

4.1.1. Shrub lithofacies

Description: The shrubs, identified by Chafetz and Folk (1984) started as branches that radiated upward to form colonies. Guo and Riding (1998) also described shrubs as little bush-like structures that are mainly common precipitations on parallel to subparallel surfaces and later, Chafetz and Guidry (1999) divided shrubs into “bacterial shrubs”, showing very irregular forms, “crystal shrubs” and “ray-crystal crusts” displaying regular geometric patterns. In this study, under the microscope, individual shrub layers are formed in different crystal shapes of branches (Figures 3a–3c). Shrubs are bounded by the micritic layer and are generally very well observed in thin sections (Figures 3d–3f). The radial dendritic shrub structure is a spherical lump formed of dark micritic filaments and twigs (Figures 3e and 3f). These shrubs are filled with microspars and radial bush structures resemble a fan. Radial micritic filaments and twigs thicken from the center outwards. The other shrub morphotypes are feather-like crystal shrubs. Erosional surfaces commonly bound shrub layers with lithoclast fragments.

Interpretation: Bacterial activity changes the environment to alkaline by increasing the pH through photosynthesis. Due to the carbonatization and depletion of the cyanobacteria, which are among these micritic feather-like structures, the pH decreases, and the spar calcite crystals precipitate. The shrub travertine facies are interpreted in different environmental conditions by several researchers (Chafetz and Folk, 1984; Guo and Riding, 1998; Minissale and Sturchio, 2004; Faccenna et al., 2008; Wright, 2012; Chafetz, 2013; Claes et al.,

2017; Erthal et al., 2017). The shrub forms of the Bahçecik travertines are developed in both shrub-flat (depression depositional) and terrace pool facies (slope depositional systems) (Figures 2b and 2c).

4.1.2. Crystalline crusts lithofacies

Description: The crystalline crusts are observed as dark and light laminae layers in the investigated travertine (Figures 2e and 4d). Crystalline crusts are usually formed as dense, compact calcite layered and they are from a few centimeters to tens of centimeters in thickness. The calcite crystals are composed of feather-like compositions formed with syntaxial growth. This lithofacies is very well observed in the middle part of the D section and is generally associated with wavy lamination and coated gas bubbles (Figure 5).

Interpretation: The deposition of crystalline crusts typically characterizes a slope environment in which thin to very thin sheets of hydrothermal water move with a laminar regime forming feather-like laminae (Guo and Riding, 1998; Gandin and Capezzuoli, 2008). Locally, crystalline crust layers are deposited on inclined surfaces from fast-flowing waters with rapid CO₂ degassing (Jones and Renault, 2008). The remains of microbial filaments represented bacterial colonization, and play an important role in developing these lithofacies.

4.1.3. Reed lithofacies

Description: The plant stems and growing branches upward in travertine precipitations are generally studied as “reed” type travertines (Guo, 1993; Guo and Riding, 1998). This lithofacies is observed in the upper levels of the Bahçecik travertines quarry. The reeds are branched and extended vertically upwards, which reached up to 15 cm long (Figure 2i). The amount of organic matter and the void ratio are higher in dark-colored reed travertines than other types of travertine. The diameter of the molds left by the plant stems and roots is at most 1–3 cm (Figure 4e). The lithofacies is associated with the laminated (micritic) travertines.

Interpretation: Reed lithofacies is observed in widespread depositional settings such as pool and slope (Guo and Riding, 1998; Jones and Renault, 2010). Reeds and various aquatic plants mostly grow in shallow depression depositional environments, where hot water is diluted with meteoric water. In the Bahçecik travertines quarry, the reed mound depositional environment is the wetlands, where large grasses have assembled in the depression areas. The reeds are common components of very shallow, occasionally drying flat lands such as swamps.

4.1.4. Laminated (micritic) lithofacies

Description: Lamination is the most common lithotype in travertine occurrences and comprises of dense laminae form mms to cms thick. Lamination occurs due to the alternation of the micritic layer. The laminae, which both light and dark (yellowish to brown) colored are observed as horizontally bedded in the F section. Wavy lamination is detected in the middle and upper parts of the D section (Figure 5).

Interpretation: The assemblages of laminae are frequently the result of daily/seasonal growth rhythms (Pentecost, 2005). Micritic layers are almost widespread lithotypes in travertines

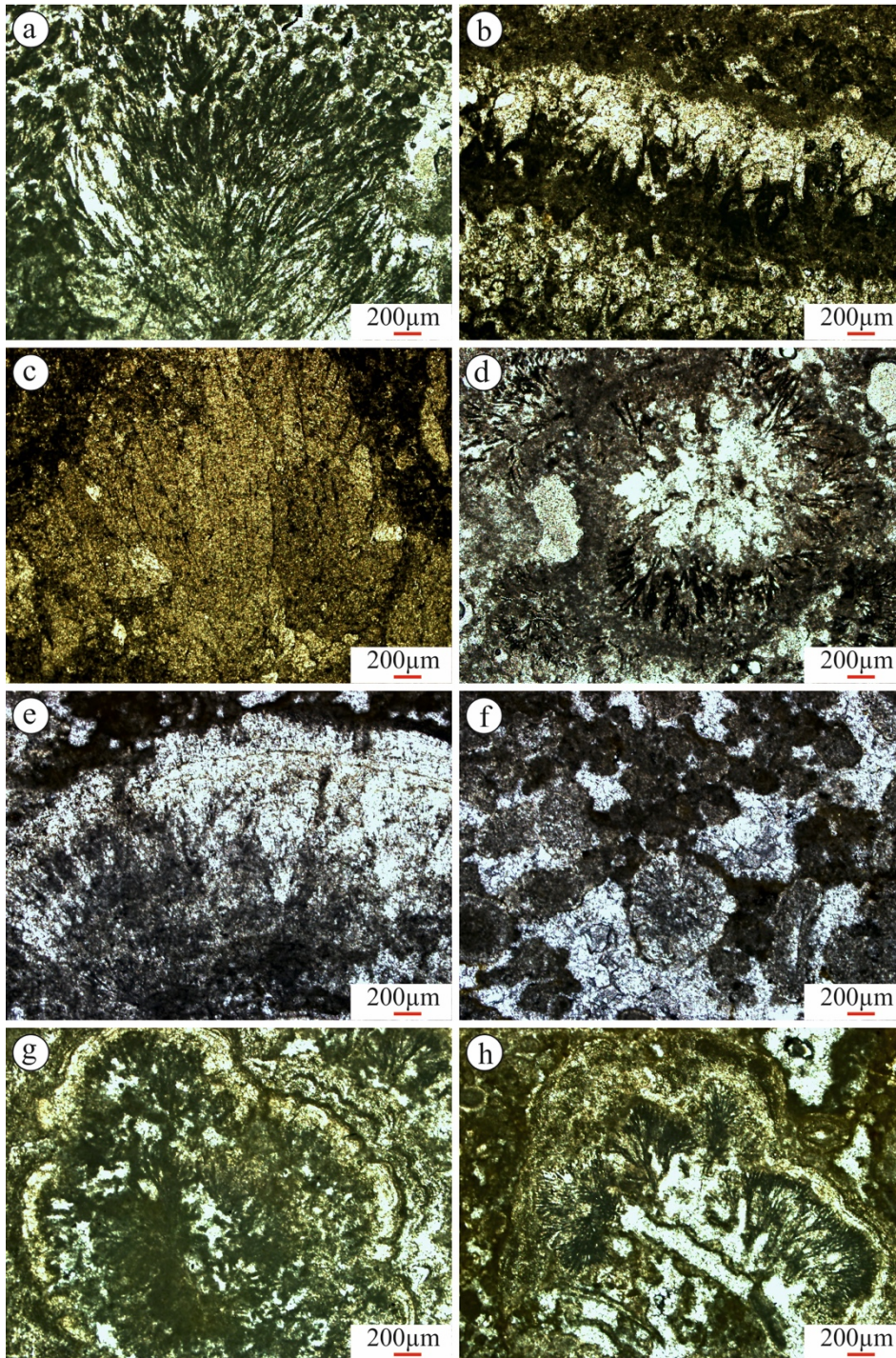


Figure 3. The microscopic images of shrub morphotypes from the Bahçecik travertines. (a) Illustrate the dendritic shubs (sample no: D-22); (b) Shrub-like morphology consisting of alternating micrite and sparite laminae, where internally branches can be observed (sample no: D-19); (c) Narrow fan shaped shub (sample no: D-15); (d) Spheroid rosette of radial dendritic shubs (sample no: F-22) (scale 200 μm); (e) Fan shaped shub (sample no: F-23); (f) Amalgamated spheroidal shubs (sample no: F-2); (g and h) Thin layered light and dark laminae and internally radial shubs (sample no: F-8) (scale 200 μm).

(Jones and Renaut, 2010). The horizontal micritic layers could be developed in flat pool facies in association with microbial mats. On the other hand, wavy lamination represents pools of terraced slope systems and inclined slope surfaces associated with fast-flowing crystalline crust.

4.1.5. Pisoid lithofacies

Description: Pisoids are common lithotype in travertine occurrences. The sizes of the pisoids vary from a few mm to 1–2 cm. A micritic coating bounds pisoids and concentrically laminated micrite/sparite interlaminae (Figure 4b), and are distinguished under three types in the microstructure: a)

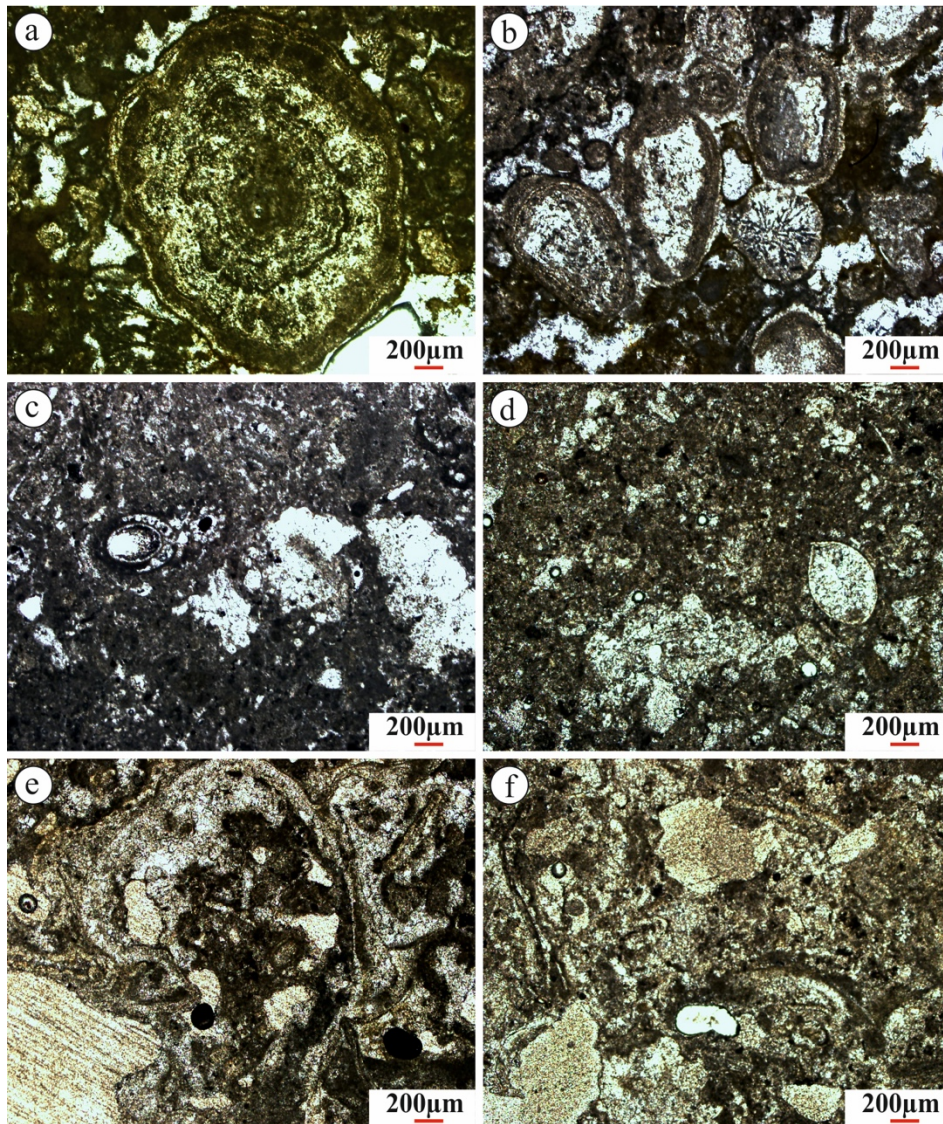


Figure 4. The microscopic images illustrating the lithofacies/lithotypes in the Bahçecik travertines. (a) oncoïd (prolate spheroidal) (sample no: F-3); (b) pisoids with spheroidal shrub (sample no: F-3); (c) Charophytes in micritic travertine (sample no: F-25); (d) Ostracod fragment in micritic travertine (sample no: F-5); (e and f) Lithoclast fragments with coated filaments in micritic travertine (sample no: F-20 and F-22).

concentric laminated, b) dendroids (radial shrub) c) stromatolitic type pisoids. Pisoids are mostly observed in the F section and significantly detected in thin sections (Figure 4).

Interpretation: Pisoids may form in the different depositional environments from small terrace pools on steep slopes associated with pebbles/micrite to large pools in depression areas (Guo and Riding, 1998; Jones and Renault, 2010). The concentrically laminated pisoids have been interpreted as being formed in turbulent water and regarded as inorganic precipitates (Folk and Chafetz, 1983; Guo and Riding, 1998; Barilaro et al., 2012). Dendroids have a distinct dendritic microstructure. The recent travertine precipitations in Italy (Terme San Giovanni) show that dendroids are formed in moderately agitated microterrace pools. Radial dendroids are formed abiotically in stagnant waters, while concentric laminas are formed by microbial effects in flowing

water (Rainey and Jones, 2005). Radial dendroids are branching surfaces that grow around the nucleus in stagnant waters and are represented by rapid crystallization. Similar coated grains (pisoids) have also been reported in Denizli, SW-Turkey (Pamukkale, Aksaz and Çukurbağ, etc.; Özkul et al., 2013), Konya, central Turkey (Kavakköy travertine; Karaisalioglu and Orhan, 2018).

4.1.6. Oncoid lithofacies

Description: Oncoids are composed of algae enveloped with varying thickness and structure of micrite, developing around a nucleus (Pentecost, 2005). The oncoïd nucleus is not apparent due to recrystallization or planar transition direction. However, the nucleus may often be different small algal carbonate aggregates. Algal coats are of irregular thickness and have a wavy structure. Moreover, oncoïds have

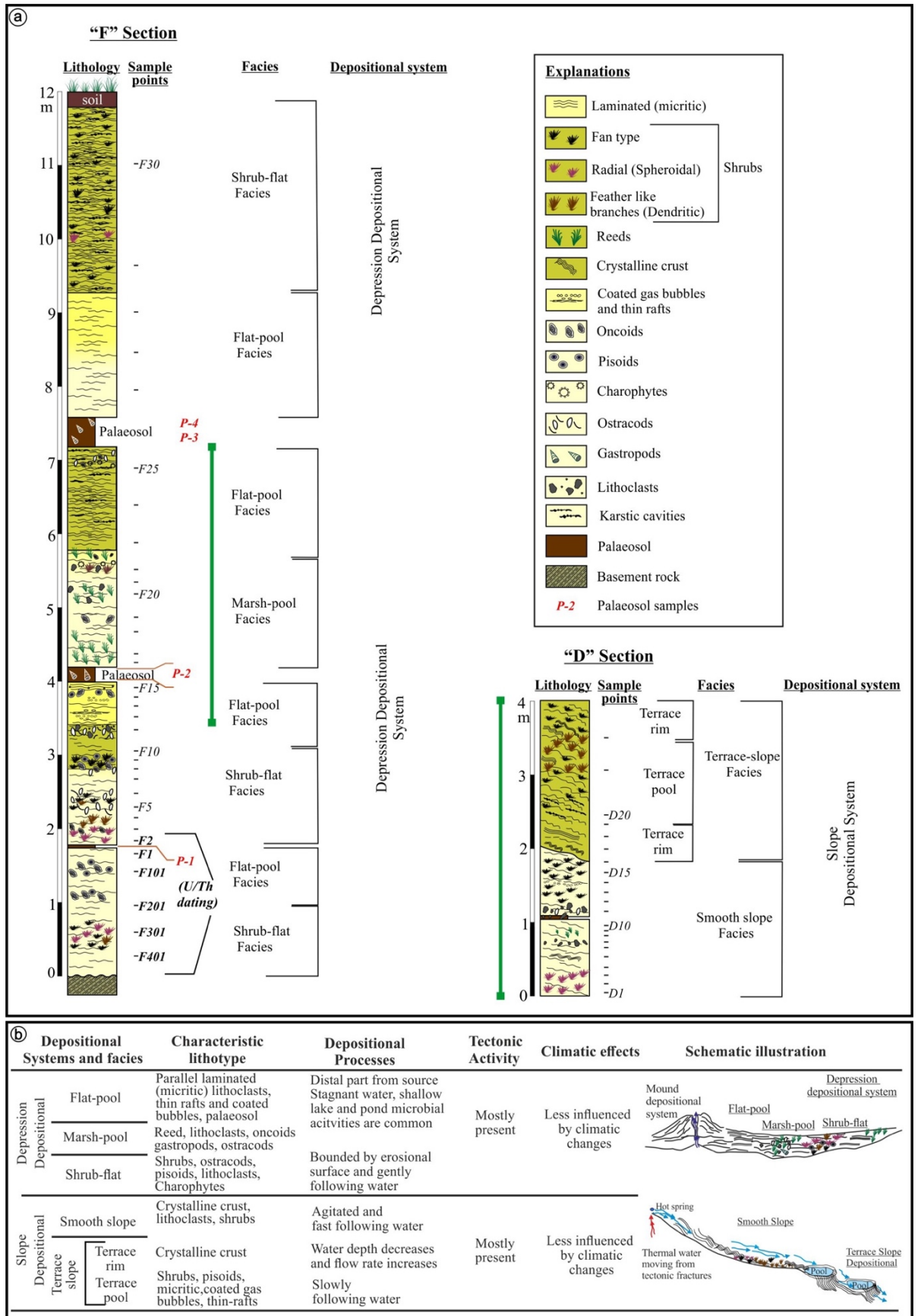


Figure 5. (a) Measured stratigraphic sections from the Bahçecik travertine quarry (F and D sections) and (b) Schematic illustration of lithofacies and depositional systems of the Bahçecik.

a micritic structure and sometimes consist of thin psedospars. Oncoids are mostly observed in the F section, particularly beneath of the palaeosol levels, and they are associated with pisoids (Figure 5).

Interpretation: Oncoids formed in travertine are commonly found in streams, rivers, and freshwater lakes (Pentecost, 2005). The size of oncoids strongly depend on water depth in the lacustrine environment and thus, oncoid size increases when getting deeper into water (Shäfer and Stapf, 1978; Jones and Wilkinson, 1978). On the other hand, the shape of the oncoid gives quite an important clue for the rate of movement. If the movement rate is high, fluvialite oncoids (mostly prolate spheroids) develop (Pentecost, 2005). In the investigated travertines, the shapes of oncoids are quite variable. These facies could be formed in the pools separating travertine dams, often being washed down to the next pool (Braithwaite, 1979).

4.1.7. Coated gas bubbles and thin rafts lithofacies

Description: The coated bubbles form as subspherical to circular or elongated micritic/microsparitic coatings around porous structures with a diameters ranging from mm to a few cm. Rafts are mostly thin and semitransparent. Generally they associate with coated gas bubbles (Figures 2f, 2g and 4d). They are characterized by whitish-beige colored, thin, delicate, brittle and flat crystalline layers. Coated bubbles and thin calcite rafts are mostly observed in the middle part of the F section and lower part of the D section (Figure 5).

Interpretation: The rafts are calcium carbonate crystalline layers, which precipitate at the water surface usually inside terraces or hot water bodies with the low flow velocity. These thin rafts could be interpreted to reflect slow-flowing water rates that consequently support stagnant conditions. Coated gas bubbles mostly form near pool surfaces below rafts or among crystals or vegetation in pools and porous sediments, where bubbles are trapped (Guo and Riding, 1998; Özkul et al., 2002). These bubbles are mainly developed from microbial activity in underlying sediments. Consequently, coated gas bubbles are commonly rafts in terrace pools (Kele et al., 2011; Özkul et al., 2013).

4.1.8. Lithoclast

Description: Lithoclasts are grey to light brownish colored lithified carbonates and mostly composed of silt-sand size detrital. The size of the clasts is about 1–1.5 cm and they are generally poorly sorted. Their shapes vary from angular to subangular. The structures in which the angular shapes are located are micritic grains formed by fragmentation of microbial micrite structure and facies (Figures 2e and 2f) (Turhan, 2007). Lithoclast fragments within the depositional area are most probably derived from limestones from around the study area and the fragmentation and displacement of semicompacted carbonate sediments. In the studied travertine sections, lithoclasts are commonly observed in both sections (Figure 5).

Interpretation: Lithoclastic material transportation results from the erosion of travertine and are incorporated into detrital fragments derived from carbonate rocks located in the surrounding area. The reason for erosion could be intensively

related to the interruption of the thermal water flow or changes in its direction (Gandin and Capezzuoli, 2014; Cook and Chafetz, 2017). In the investigated area, lithoclasts are represented in marsh-pool facies of depression depositional and smooth slope systems (Figure 5).

4.1.9. Palaeosol

Description: The palaeosol levels are composed of brown-colored, mud-rich detritals, ranging from a few cm to 30 cm in thickness (Figure 5). Although these clastic levels are not directly travertine lithofacies, they are closely related to the lithofacies. Palaeosols are frequently observed in intermediate levels and the Bahçecik quarry faces and can be followed along the erosional surface through the tens of meters. Some paleokarstic cavities are commonly observed. Gastropod fragments are observed locally (Figures 2h and 5). In the F section of the Bahçecik travertines quarry, 2 different palaeosol levels have been detected (Figure 2b). Horizontally laminated travertines levels are generally observed at the bottom of palaeosol layers (Figure 5).

Interpretation: Palaeosols are strongly related to the erosional surfaces of travertine deposits. Erosional surfaces crop out when a fall of the water table or a deviation of water flow direction occurs. Palaeosol or soil formations overlie these erosional surfaces and are generally observed between travertine sequences. They are mostly rich in faunal and floral aspects. Depending on any water flow direction changes, subaerial desiccation and biological activities associated with soil formation can occur. The soil formation is mainly composed of mud, silt, and sand detritals accumulate on the erosional surface. Erosion surfaces and overlying palaeosol layers in the investigated travertine site are represented in pool settings of depression depositional systems (Figure 5).

4.2. Depositional systems

In this study, two different depositional systems have been recognized; slope depositional and depression depositional systems. The depression depositional system is subdivided into three depositional subsystems: shrub flat, marsh-pool, and flat-pool facies. All these subsystems have developed in shallow pools related to mostly stagnant water with agitation in some levels.

4.2.1. Slope depositional system

A slope depositional system commonly develops like a smooth slope with terrace parts. The angles of slope surfaces are from 20° to 45°. This depositional system is observed in the travertine quarry (Figures 4 and 5). The most common lithotype is a crystalline crust of the slope depositional system. Moreover, wavy lamination can be easily recognized. The slope depositional system is laterally and vertically associated with the depression depositional system.

The Bahçecik travertine, particularly the upper part of the D section has been precipitated in smooth slope facies and terrace slope facies divided by terrace rim and pool (Figures 5a and 5b).

4.2.2. Depression depositional system

4.2.2.1. Shrub flat facies

Guo and Riding (1998) first used the term shrub flat facies for light-colored, thin-bedded horizontal or nearly horizontal

bushes travertine deposits. According to Guo and Riding (1998), shrub forms, which are the usual component of terrace ponds, are the most common and thick travertine lithofacies of shallow pool and swamp-like environments in depression areas.

This depositional system is mainly characterized by laminated (micritic), gas bubbles lithotypes and palaeosol layers. The shrub flat facies usually occur in the terrace pool (Toker et al., 2015).

4.2.2.2. Marsh-pool facies

The term marsh-pool facies has been used by Guo and Riding (1998) for reed and pebbly travertines varying from gray to brown-colored. Swamp-pond sediments are commonly associated with shrub-flat facies and generally darker, brown brecciated levels are observed in the Bahçecik travertines. The travertines in this studied area are brown voided and have a high organic matter content. Gastropods are common in these facies. These sediments have been deposited in shallow lake or pool environments. This facies has been stated for Kocabaş travertines (Denizli-SW Turkey) occurrences (Toker et al., 2015).

4.2.2.3. Flat-pool facies

Flat-pool facies develop in the shallow pool and are most probably fed by subaqueous springs upwelling along the faults and fractures (Chafetz and Folk, 1984; Guo and Riding, 1998; Facenna et al., 2008; Özkul et al., 2013; Toker et al., 2015). Generally, shrubs are a common lithotype in the depression depositional system, but parallel lamination (horizontal bedded) is common in this studied travertine face. The parallel lamination might be followed through lateral continuity from tens to a hundred meters. These facies are commonly characterized by the wavy transitions of light and dark laminae. This transition in color and density may be due to seasonal changes and algal filaments (Toker et al., 2015). Whitish levels may precipitate major chemical functions, while dark levels are related to organic matter content. Whilst dark laminae are more porous, whitish parts are more compact and rarely porous. The other characteristic lithotypes are lithoclasts, thin rafts, coated gas bubbles, palaeosols in the Bahçecik travertines.

4.3. ^{230}Th ages

In this study, uranium and thorium isotopic compositions and contents and ^{230}Th ages are summarized in Table 1 from two sections of the Bahçecik travertines. The new geochronological dates from two sections (F and D) in the Bahçecik travertines yielded ages between 353 ka and 264 thousand years ago (ka, relative to 1950 AD) (Table 1). The dating records indicate that the Bahçecik travertine precipitations formed in the middle Pleistocene.

According to age results, the Bahçecik travertines commenced to precipitate at MIS 10 (glacial) and continued to accumulate during the MIS 9 (interglacial) and MIS 8 (glacial) periods.

4.4. Stable isotopic records

Stable isotopic carbon and oxygen values obtained from terrestrial carbonates are used to provide information about the environmental conditions of the precipitation processes (Andrews, 2006). Totally, 54 (F1-28; F101-104 and D1-22)

travertine bulk samples were systematically collected from two sections (F and D sections in Figure 5). Accordingly stable isotope values from two sections of the Bahçecik travertines are given in Table 2.

According to new stable isotopic records of these terrestrial carbonates, $\delta^{13}\text{C}$ values range from +3.25 ‰ to +6.01‰ (V-PDB) while $\delta^{18}\text{O}$ values are between -14.67 ‰ and -12.64 ‰ (V-PDB).

Depending on these results, positive $\delta^{13}\text{C}$ values indicate that the Bahçecik travertines are most probably thermogenic in origin (Pentecost, 2005).

4.5. Palynomorphs

Palaeosol samples (P1, P2, P3 and P4) from the Bahçecik travertines obtained from F and D sections are all virtually barren in palynomorphs, except a few sporadic pollen grains. Palynomorphs of all samples represent by 1 taxa of the gymnosperm pollen and 3 taxa of the angiosperm pollen. Moreover, *Glomus* of the nonpollen palynomorphs, cuticle, and zooclasts are also recorded in the samples. The P1 sample is characterized by Pinaceae-*Pinus* (90%) and Fagaceae-*Quercus* evergreen type and *Quercus* spp. (10%), and abundant cuticle pieces (40%). The P3 sample consists of Pinaceae-*Pinus* (70%) and Fagaceae-*Quercus* evergreen and *Quercus* spp. (15%). Additionally, herbaceous plants Asteraceae-Asteroideae and -Cichorioideae (15%) and Poaceae (1%) are also recorded in the P3 sample. The P4 sample includes Fagaceae-*Quercus* evergreen and Asteraceae-Asteroideae and -Cichorioideae. *Glomus* remains the most abundant nonpollen palynomorph.

4.6. GPR interpretation

This study embodies the process in which the collected GPR data was made ready for interpretation by applying the data processing steps. When the radargrams were analysed in general terms, reflections from a depth of approximately 12–14 m were obtained in the measurements performed in the N-S direction with a 100 MHz unshielded antenna (Figure 6a).

The current study has also enabled the determination of the existing discontinuities in the Bahçecik travertine terraces, the thickness of the travertine, the tectonic structures they include, as well as their sedimentary properties (Figure 6b). The quarry slope is located in the Bahçecik travertines. The different levels that can be separated from the bottom to the top within the travertine sequence and the palaeosol levels are observed between them (Figure 6b). Moreover, the measured stratigraphic section (F section) is obtained from the travertine quarry (Figure 5). The travertine projections in the radargram can be correlated with those in the F section (Figure 4). It was also observed in 100 MHz GPR radargrams that were applied that the travertine sequence consists of two primary levels and that these two levels are divided into two parts by an old soil level (palaeosol) of 50 cm in thickness, found at approximately the 7th m of the sequence (Figure 6a). These two different levels in the travertine sequence are also different in terms of both appearance and characteristics. The company mentioned above has mostly operated from the lower levels of the quarry. In the studies carried out, the travertines of the sequence, which were up to 7 m, were more compact and less porous than the upper ones. Besides, there

Table 1. Uranium and thorium isotopic compositions and ^{230}Th ages for travertine carbonates by MC-ICPMS, Thermo Electron Neptune, at HISPEC, NTU. Sample points are indicated in Figure 5.

| Sample ID | Weight g | ^{238}U 10^{-9}g/g^a | ^{232}Th 10^{-9}g/g | $d^{234}\text{U}$ measured ^a | $[\text{}^{230}\text{Th}/\text{}^{238}\text{U}]$ activity ^c | $^{230}\text{Th}/\text{}^{232}\text{Th}$ atomic ($\times 10^{-6}$) | Age (year ago) uncorrected | Age (year ago) corrected ^{c,d} | Age (year BP) relative to 1950 AD | $d^{234}\text{U}_{\text{initial}}$ corrected ^b |
|-----------|----------|--|---------------------------------------|---|--|--|----------------------------|---|-----------------------------------|---|
| F2 | 0.0610 | 532.31 ± 0.70 | 413.6 ± 7.6 | 403.8 ± 2.1 | 1.402 ± 0.040 | 29.7 ± 1.0 | 275.551 ± 29299 | 263.927 ± 27386 | 263.856 ± 27386 | 851 ± 75 |
| F1 | 0.0544 | 559.95 ± 0.70 | 376.0 ± 6.2 | 396.1 ± 2.1 | 1.404 ± 0.040 | 34.5 ± 1.1 | 283.710 ± 31894 | 273.769 ± 29885 | 273.698 ± 29885 | 858 ± 84 |
| F101 | 0.0556 | 400.05 ± 0.53 | 101.0 ± 1.1 | 398.8 ± 2.0 | 1.405 ± 0.021 | 91.7 ± 1.7 | 282.009 ± 16214 | 278.396 ± 15862 | 278.325 ± 15862 | 875 ± 43 |
| F201 | 0.0621 | 468.84 ± 0.59 | 75.27 ± 0.69 | 365.7 ± 2.1 | 1.378 ± 0.021 | 141.5 ± 2.5 | 293.334 ± 18297 | 290.994 ± 17996 | 290.923 ± 17996 | 831 ± 47 |
| F301 | 0.0491 | 510.13 ± 0.60 | 28.45 ± 0.14 | 351.7 ± 1.9 | 1.388 ± 0.010 | 410.5 ± 3.6 | 319.936 ± 11391 | 319.143 ± 11326 | 319.072 ± 11326 | 866 ± 30 |
| F401 | 0.0552 | 729.4 ± 1.2 | 100.7 ± 1.0 | 324.1 ± 2.4 | 1.381 ± 0.019 | 164.8 ± 2.7 | 355.216 ± 28661 | 353.256 ± 28226 | 353.186 ± 28226 | 878 ± 81 |

Analytical errors are 2σ of the mean.

^a $[\text{}^{238}\text{U}] = [\text{}^{235}\text{U}] \times 137.818 (\pm 0.65\%)$ (Hiess et al., 2012); $\delta^{234}\text{U} = ([\text{}^{234}\text{U}/\text{}^{238}\text{U}]_{\text{activity}} - 1) \times 1000$.

^b $\delta^{234}\text{U}_{\text{initial}}$ corrected was calculated based on ^{230}Th age (T), i.e. $\delta^{234}\text{U}_{\text{initial}} = \delta^{234}\text{U}_{\text{measured}} X e^{\lambda^{234}T}$, and T is corrected age.

^c $[\text{}^{230}\text{Th}/\text{}^{238}\text{U}]_{\text{activity}} = 1 - e^{-\lambda^{230}T} + (\delta^{234}\text{U}_{\text{measured}}/1000)[\lambda_{230}/(\lambda_{230} - \lambda_{234})](1 - e^{-(\lambda_{230} - \lambda_{234})T})$, where T is the age.

Decay constants are $9.1705 \times 10^{-6} \text{ year}^{-1}$ for ^{230}Th , $2.8221 \times 10^{-6} \text{ year}^{-1}$ for ^{234}U (Cheng et al., 2013), and $1.55125 \times 10^{-10} \text{ year}^{-1}$ for ^{238}U (Jaffey et al., 1971).

^dAge corrections, relative to chemistry date on May 27th, 2020, were calculated using an estimated atomic $^{230}\text{Th}/\text{}^{232}\text{Th}$ ratio of $4 (\pm 2) \times 10^{-6}$.

Those are the values for a material at secular equilibrium, with the crustal $^{232}\text{Th}/\text{}^{238}\text{U}$ value of 3.8. The errors are arbitrarily assumed to be 50%.

Table 2. The stable isotopic values from F and D sections of the Bahçecik site (Gümüşhane). Sample points are indicated in Figures 5 and 7.

| Sample name "F" section | $\delta^{13}\text{C}$ (V-PDB) | $\delta^{18}\text{O}$ (V-PDB) | Sample name "D" section | $\delta^{13}\text{C}$ (V-PDB) | $\delta^{18}\text{O}$ (V-PDB) |
|----------------------------|----------------------------------|----------------------------------|----------------------------|----------------------------------|----------------------------------|
| F401 | 4.81 | -14.17 | D1 | 4.85 | -13.79 |
| F301 | 5.00 | -14.6 | D2 | 4.8 | -13.95 |
| F201 | 4.87 | -14.62 | D3 | 5.11 | -13.53 |
| F101 | 4.5 | -14.67 | D4 | 5.15 | -13.72 |
| F1 | 5.15 | -14.02 | D5 | 4.8 | -13.46 |
| F2 | 4.81 | -14.21 | D6 | ----- | ----- |
| F3 | 4.67 | -13.33 | D7 | ----- | ----- |
| F4 | 4.72 | -14.3 | D8 | 4.6 | -13.7 |
| F5 | 4.93 | -14.45 | D9 | 4.64 | -13.73 |
| F6 | 5.33 | -14.34 | D10 | 5.01 | -13.49 |
| F7 | ----- | ----- | D11 | 6.29 | -13.43 |
| F8 | ----- | ----- | D12 | 6.53 | -13.45 |
| F9 | 4.61 | -14.12 | D13 | 5.77 | -13.43 |
| F10 | ----- | ----- | D14 | 5.61 | -13.44 |
| F11 | ----- | ----- | D15 | 5.78 | -13.7 |
| F12 | 5.28 | -14.47 | D16 | 6.01 | -13.5 |
| F13 | ----- | -13.57 | D17 | 5.88 | -13.12 |
| F14 | 4.18 | -13.83 | D18 | ----- | ----- |
| F15 | 3.46 | -13.72 | D19 | 5.43 | -14.09 |
| F16 | 3.25 | -13.74 | D20 | 5.16 | -14.01 |
| F17 | ----- | ----- | D21 | 4.73 | -13.26 |
| F18 | 3.57 | -13.28 | D22 | 4.71 | -13.51 |
| F19 | 3.54 | -13.44 | | | |
| F20 | 3.59 | -13.19 | | | |
| F21 | 3.81 | -13.25 | | | |
| F22 | 3.72 | -13.43 | | | |
| F23 | 3.73 | -13.15 | | | |
| F24 | 3.66 | -13.07 | | | |
| F25 | 3.52 | -12.64 | | | |
| F26 | 3.53 | -12.76 | | | |
| F27 | ----- | ----- | | | |
| F28 | 3.87 | -12.81 | | | |

were also old soil layers that appear at different levels between 0 and 7 m of the sequence, extending lenticular in a lateral direction from time to time. The layer of the sequence above the palaeosol level was observed to be highly porous and with cavities, hence less monolithic compared to the lower levels. This layer mainly consists of travertines described as highly porous tufa, containing a variety of plant parts, including stems. The high amplitude reflections represent the karstic cavities structure within the travertines. In Figure 6b, some reflective boundaries within the Late Cretaceous aged Kermutdere Formation of a depth of 12–19 m were observed. These boundaries are thought to have maybe been on

different lithological levels within the turbidites. While the dominant lithology within the Kermutdere Formation observed under the Bahçecik travertine terraces consists of the intercalation of sandstone-claystone-marl, conglomerate and tuff levels that are also observed within the section at intermediate levels.

5. Discussion

In this study, Bahçecik travertine terraces, which are found to precipitate in depression depositional and slope depositional systems during middle Pleistocene in Gümüşhane, NE-Turkey were collected and analysed. Thus, the first findings obtained from these terrestrial carbonates in NE-Turkey have been explicitly stated considering depositional systems according to the facies description and interpretation, radiometric dating, stable isotopes, palynomorphs, and also geophysical results. All the results obtained from these multidisciplinary analyses were correlated with each other and compared with other significant terrestrial outcrops representing in the Quaternary period.

5.1. Palaeoenvironmental development

Bahçecik travertines were deposited within the depression depositional (shallow pool setting) and slope depositional systems. During the precipitation process, the travertine deposition occasionally ceased due to tectonic events and climatic changes, and thus, palaeosol levels developed. In this multidisciplinary study, the radiometric age, stable isotope data, and palynomorphs were systematically obtained from the travertine terraces of Bahçecik. The climatic change and tectonic activity in this region during the Quaternary period had a significant effect on the development of the sediments. Bahçecik travertines were determined to have considerably negative $\delta^{18}\text{O}$ values; on the other hand; the $\delta^{13}\text{C}$ isotope values are quite positive. The positive results in carbon values have demonstrated that thermal waters come out to the surface from deep fractures and cracks in carbonate rocks, which then enter these travertines. The fluctuation of oxygen values could be related to climatic changes. The stable carbon isotope data of Bahçecik travertines (typically -3 to $+8\%$ V-PDB) reveal that these travertines are thermogenic (Pentecost, 2005). Furthermore, the very low $\delta^{18}\text{O}$ values are related to poor evaporation stage and relatively high water temperatures (Andrews et al., 1997).

According to the age data obtained from the bottom part of the F section, these travertines started to precipitate at approximately 353 ka (MIS 10) in the glacial period; and later, a travertine sequence with a thickness of 1.5 m deposited in between 319 ka and 278 ka (MIS 9). The presence of oxygen values leading to a negative increase from this bottom part of the section (-14.17 to -14.67% V-PDB; Table 2) suggests that meteoric waters were mixed into the environment. As a result of sedimentological studies, it has been revealed that the travertines in this interglacial period may have precipitated in a shallow pool setting with abundant shrubs and partly turbulent structure (with the presence of pisoids and oncoids) (Figure 7). The travertine deposition ceased during the transition to the glacial period at approximately 273 ka (MIS 8), and palaeosol level of 20–25 cm was formed (Figure 7). In

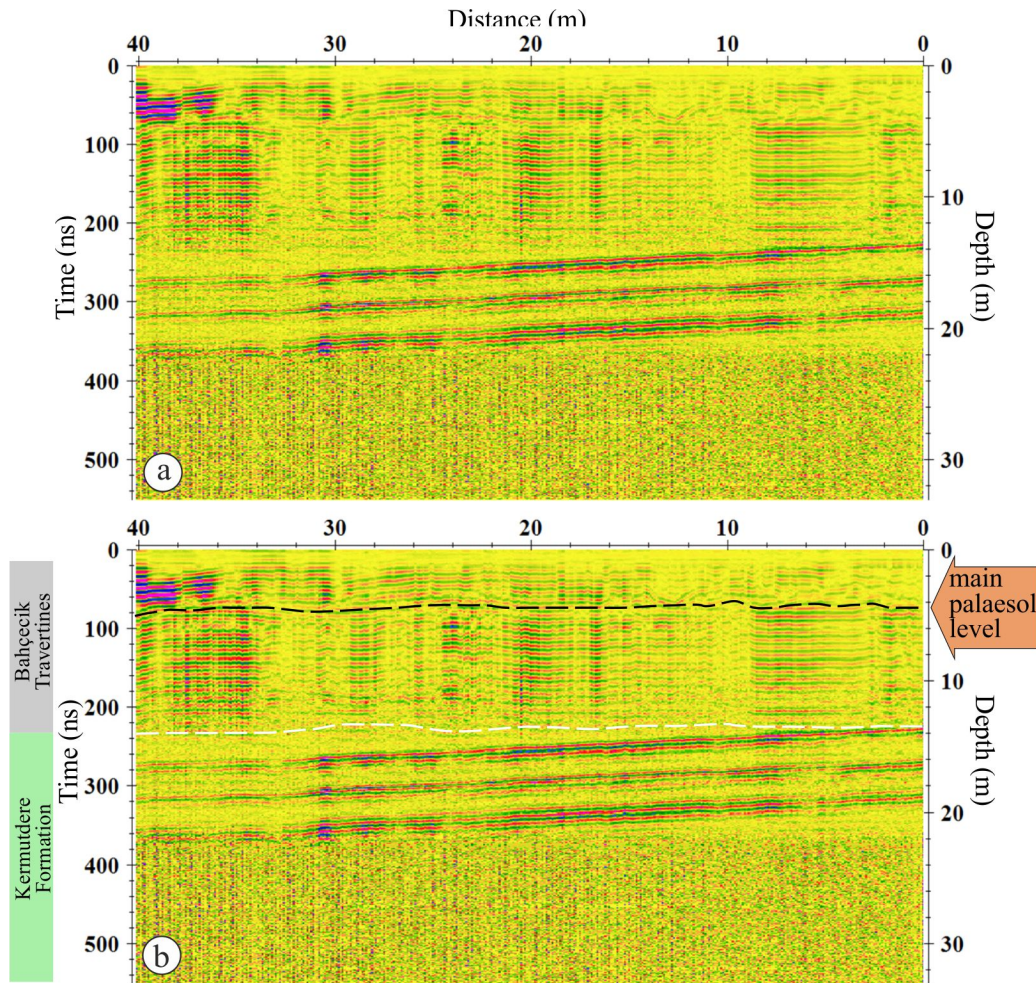


Figure 6. (a) Original and (b) processed radargram with 100 MHz antenna on the upper side of quarry in a north to south direction.

palynological studies conducted at palaeosol levels (P1), very many cuticles, which are epidermal tissue of higher plants, were defined (Mendonça-Filho et al., 2012). It can be argued that these cuticles could have probably entered the bodies of palaeosols by the disintegration and transference of shrubs during the precipitation of these palaeosols. Also, unbroken and large appearance of these cuticles indicates that they have been transferred from a short distance away. The abundance of gymnosperms shows that there are middle and high-altitude areas around the deposition area. Travertine deposits could be precisely detected in the glacial period around 263ka (MIS 8) according to limited age data. However, significant changes of stable isotopic values have been clearly observed in whole sections.

The following precipitation period ceased with the second palaeosol level after approximately 2.20 cm (Figure 5). This sedimentary sequence of the F section, starts with a density of radial and dendritic shrubs. Towards the middle of the sequence, it turns into a level where ostracods are abundantly observed (Figure 7). The overlying pisoids and oncoids indicate the existence of a slightly turbulent and temperate environment in the shrub-flat facies. The second palaeosol level, which starts with ostracod shells and lithoclasts approximately 1-m-thick, then continues with coated gas

bubble/paper thin raft and pisolites, has deposited in the flat-pool facies (Figure 7). In the stable isotope data collected from this second sequence, a decreasing at carbon values and relatively increasing at the oxygen values was recorded (Figure 8). The slightly increasing of values (-14.21 to -13.72 ‰V-PDB; Table 2) could be related to a warming in climate and ambient water evaporation. This climatic aridity may have caused an interruption of carbonate precipitation and in the meantime the palaeosol level containing rich organic detritals and gastropod fragments may have developed. However, all the samples examined in the palynological analyses collected from the second palaeosol level (P2) were completely barren.

The next sequence of F section is an approximately 4 m thick travertine deposit and middle part of the sequence is characterized by plenty of reeds, intercalated with pisoids. In the upper part of the section, charophytes are commonly observed (Figure 7). According to the lithofacies analysis, this travertine sequence in the F section was deposited in the marsh pool facies with abundant reeds and relatively shallow water level, which is slightly turbulent (presence of pisoids). While there is no significant change in carbon values in stable isotope data in this sequence range, oxygen values continue to increase relatively (-13.74 to -12.64 ‰V-PDB; Table 2). The

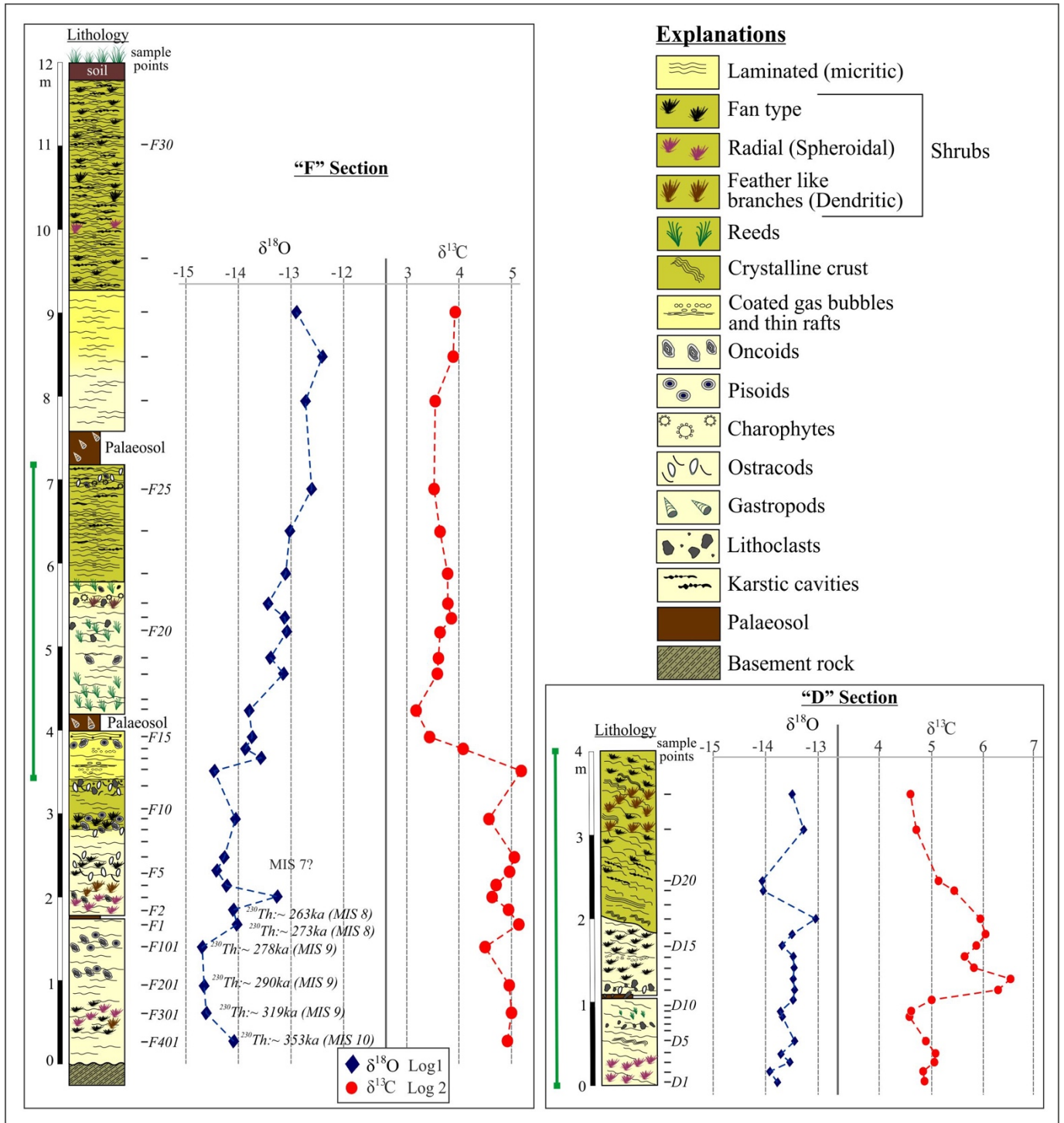


Figure 7. F and D measured stratigraphic sections with oxygen and carbon isotope curves in the study area.

palaeosol level deposited in the environment with the cessation of travertine precipitation is approximately 50 cm and contains abundant gastropod fragments like the other palaeosol levels in the lower and middle parts of the F section (Figure 7). As a result of the palynological analyses obtained from this palaeosol level (P3 and P4), the high abundance of gymnosperm pollen species indicates the presence of low and middle topographic areas in the vicinity of the sediment areas. The presence of these Fagaceae-*Quercus* evergreens, herbaceous plants (Asteraceae-Asteroidae and -

Cichorioideae and Poaceae) could be related to the warming period in the climatic condition. Additionally, the more abundance of *Glomus* (NPP) indicates the existence of erosion during the travertine deposition in the marsh pool facies.

The upper part of the F section consists of a parallel laminated travertine deposit approximately 4.5 m thick, without any shrubs or reed fragments. Significant changes in the stable isotope data were also not observed (Figure 7 and Table 2).

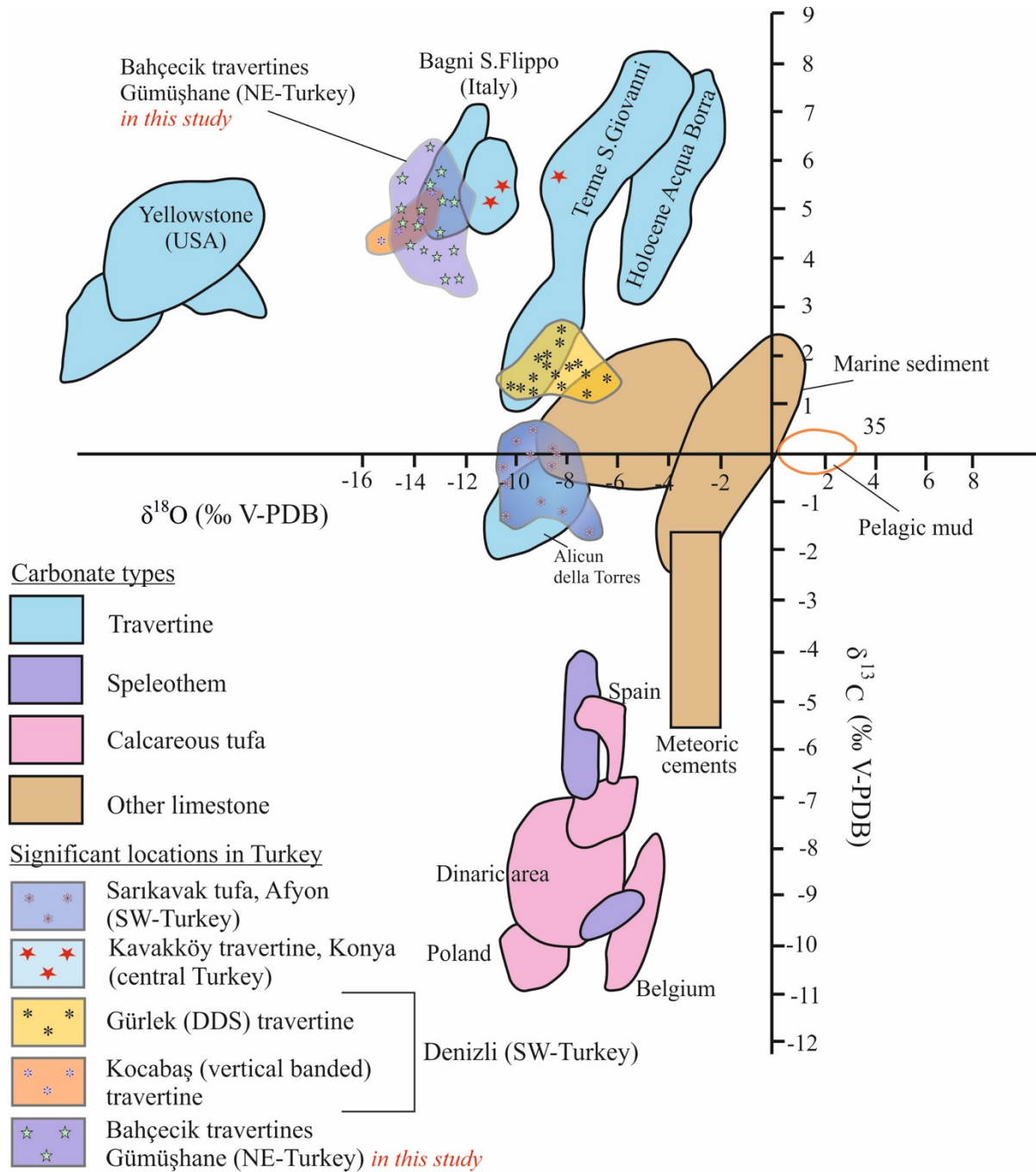


Figure 8. Combined plot of $\delta^{18}\text{O}$ (‰V-PDB) and $\delta^{13}\text{C}$ (‰V-PDB) values derived from different type of carbonates precipitated in terrestrial and marine (travertine, tufa, speleothems, marine carbonates and pelagic muds, etc.) depositional conditions and studied travertines in this study with other significant locations from Turkey (Sarıkavak tufa; Toker, 2017; Tagliasacchi and Kayseri-Özer, 2020; Kavakköy travertine; Karaisalioglu and Orhan, 2018; Gürlek and Kocabaş travertines; Özkul et al., 2013; Toker et al., 2015) (modified from Gandin and Capezzuoli 2008). DDS: depression depositional system.

The D section obtained from the Bahçecik travertines is up to 4 m and starts with dense shrubs (bushes). The first meter of sequence commences with shrubs and continue to the reeds. The analysis of the stable isotope data obtained from this sequence range shows no significant change in oxygen values but a relative increase in carbon values. The lithoclasts and ostracod fragments, just below fan-type shrubs, are observed after the sharp erosion of the 10 cm palaeosol level (Figure 5). Crystalline crust, that is a prominent structure was

precipitated in the terrace rim of the terrace-slope facies (Figures 2c–2e and 5). Lamination was also observed, which had developed depending on the gradient of the slope. When considering the stable isotope data of this level, relatively lower values of carbon and comparatively higher oxygen values, were observed. The moderately more positive (less negative) of these oxygen values could be indicative of evaporation in the depositional environment.

The GPR radargrams enabled detection of the fractured, porous, cavitied structure of the rocks at shallow depths and their stratification and lithological differences (Beres et al., 2001). In the current study, significant data was obtained concerning the propagation and discontinuities of Bahçecik travertines using 100 MHz antennas. Accordingly, the radargrams revealed that the travertine sequence is approximately 10–14 meters thick, consisting of two main sections divided by the main palaeosol level (Figures 6a and 6b). The lower part of the F section (beneath the palaeosol level; P3 and P4 samples; Figure 4a) of the Bahçecik travertine sequence seems more compact than the upper part, which is deposited in thick shrub-flat facies (approx. 3 m; Figure 4a) and flat-pool facies (approx. 1.5 m; Figure 4a) belonging to the depression depositional system. The differences of these lithofacies in the F section were observed in different radargrams (Figure 6).

5.2. Comparison with similar outcrops in the Mediterranean

The Bahçecik travertines formed in the Eastern Black Sea region are comparable with similar outcrops in the Mediterranean region (i.e. Turkey and Italy).

For instance, Denizli-Gürlek (West Anatolia) travertines deposited in a similar process (i.e. depression depositional system) like the Bahçecik travertines. However, lower stable carbon isotope values (between +2.6 and +1.3) were recorded in the Gürlek travertines (Toker et al., 2015; Figure 8). On the other hand, the values of vertical banded travertine in the Kocabaş area (Özkul et al., 2013) are quite close to the values (+4.6 and +5.6 ‰V-PDB) of the Bahçecik travertines). The carbon isotope values of Kavakköy (Konya, central Turkey) travertines precipitated in slope and depression depositional systems exist within a wide range (+0.2 and +8.2 ‰V-PDB; Karaisalıoğlu and Orhan, 2018). These high carbon isotope values are very similar to those of Bahçecik travertines (Figure 8). Similar positive values were found in the Bagni San Flippo hydrothermal travertine system in Italy (Capezzuoli et al., 2014; Della Porta and Reitner, 2020; Figure 8). The Bagni San Flippo travertines are composed of terrace ponds, where coated gas bubbles and thin rafts are widely observed near the spring (Capezzuoli et al., 2014; Della Porta and Reitner, 2020).

These highly positive values in stable carbon isotopes might also suggest that the Bahçecik travertine systems are of hydrothermal origin like Kocabaş (Denizli), Kavakköy (Konya) and Bagni San Flippo (Italy). Likewise, the abovementioned positive values indicate that the parent water is charged with CO₂ from a deep source associated with magmatic CO₂ from decarbonization of carbonate or active volcanism through thermal, magmatic, and metamorphic processes (Yoshimura et al., 2004; Pentecost, 2005; Kele et al., 2011; Teboul, 2016). When the geology of Gümüşhane and its surroundings are examined in detail, this source is expected to contain carbonate rocks belonging to the Berdiga Formation.

In addition, stable carbon isotope data obtained from the river tufa in Sarıkavak (Afyon) in western Turkey have lower values (–1.63 to +1.63 ‰ V-PDB) in comparison with the Bahçecik travertines (Toker, 2017; Tagliasacchi and Kayseri-Özer, 2020). When their oxygen isotope values were

compared, Sarıkavak tufa has more positive values than the oxygen values of the Bahçecik travertines (–7.49 and –10.78‰ V-PDB). According to the palynofloral data obtained from the palaeosol levels in the Bahçecik travertines (MIS 9 and MIS 7), the palynomorphs were low in variety even if quite rich in pollen content like the palynomorph association of the Sarıkavak tufa deposits during the same time interval (Tagliasacchi and Kayseri-Özer, 2020). A similar palynofloral association of both travertines in the western and northern Turkey was obtained and the main components of these palynofloras are Pinaceae-*Pinus*, *Quercus* evergreen type, Asteraceae-Asteroidae and Cichorioideae. However, due to the drier climatic conditions of the Sarıkavak tufa (oxygen isotope data also supports this), the diversity and the relative abundance of herbaceous forms are higher than those in the Bahçecik travertines.

6. Conclusion

The Bahçecik travertines, Gümüşhane (NE-Turkey) have been studied for the first time in terms of sedimentological, geochemical, geophysical and palynological aspects. The travertines with a total thickness around 12 m, showed massif appearance and have formed in an approximately 1 km² tectonically active area. All the results obtained through detailed field observations/studies (mapping, extraction of measured sedimentary sections and GPR study) and laboratory analyses (radiometric dating, stable isotope, palynology and petrographic) are documented:

To determine the depositional systems and facies of the Bahçecik travertines, two stratigraphic sections (F and D sections) were measured and sampled systematically for multidisciplinary analyses. Accordingly, a total of 9 lithotypes, deposited in depression depositional (shrub flat, marsh pool and flat pool facies) and slope depositional (terrace and smooth) systems, were identified.

Totally, 6 ²³⁰Th age data was determined. According to dating results, the Bahçecik travertines began to precipitate during the glacial period at approximately 353 ka (MIS 10) and continued to accumulate during 263 ka (MIS 8). The total thickness of 2 m in this 100-ka period indicates that the travertine deposition occurred very slowly.

According to the stable isotope data, significant fluctuations of oxygen values in the F section were recorded. The oxygen curve, which tending to relatively positive (less negative) values, could be strongly associated with evaporation.

Palynomorphs were detected in four palaeosol levels collected from the Bahçecik travertines and the paleoenvironmental findings based on the stable isotopes during deposition were supported by pollen identifications. Herbaceous plants (Asteraceae-Asteroidae and Cichorioideae and Poaceae) were predominantly observed in the warming period of the climate. The abundance of the *Glomus* form has been marked in especially during the processes where intense erosion is observed and during the accumulation process. This abundance also supports the idea that a process of a severe erosion phenomenon was occurring in the study area.

Different GPR radargrams have revealed that the travertine sequence is approximately 10–14 m thick, consisting of two main parts (F section) separated by the main palaeosol level. With regard to the GPR profile section, the lower part of the Bahçecik travertine sequence is more compact than the upper level, which is mostly composed of shrubs.

Acknowledgments

We are grateful to Dr. Aysel Şeren and Dr. Zeynep Öğretmen for compiling the geophysical investigations and information. Many thanks to Güven İş Marble Company (Osman Aydın) for their help during this field work and Seda Altuntaş for

language improving the manuscript. The authors also thank Anthony Bradley for checking the manuscript as a native speaker and also the three anonymous reviewers for their comments and suggestions that helped to improving the quality of this manuscript. ²³⁰Th dating was supported by grants from the Science Vanguard Research Program of the Ministry of Science and Technology (MOST), Taiwan, ROC (109-2123-M-002-001 to C.-C.S.), the Higher Education Sprout Project of the Ministry of Education, Taiwan, ROC (109L901001 to C.-C.S.), the National Taiwan University (110L8907 to C.-C.S.).

References

- Andrews JE, Riding R, Dennis PF (1997). The stable isotope record of environmental and climatic signals in modern terrestrial microbial carbonates from Europe. *Palaeogeography Palaeoclimatology Palaeoecology* 129: 171-189. doi: 10.1016/S0031-0182(96)00120-4
- Andrews JE (2006). Palaeoclimatic records from stable isotopes in riverine tufas: synthesis and review. *Earth-Science Reviews* 75: 85-104. doi: 10.1016/j.earscirev.2005.08.002
- Arenas C, Cabrera L, Ramos E (2007). Sedimentology of tufa facies and continental microbialites from the Palaeogene of Mallorca Island (Spain). *Sedimentary Geology* 197: 1–27. doi: 10.1016/j.sedgeo.2006.08.009
- Arenas-Abad C, Vazquez-Urbez M, Pardo-Tirapu G, Sancho-Marcen C (2010). Fluvial and associated carbonate deposits. In: Alonso-Zarza AM, Tanner L (editors). *Carbonates in Continental Settings: Facies, Environments, and Processes*. Developments Sedimentology 61, 1st Edition. USA: Elsevier, pp. 133–175.
- Arslan M, Kolaylı H, Temizel İ, Çiftçi İ, Alp İ et al. (2005). Petrography, geochemistry and formation conditions of Gümüşhane and Bayburt areas travertine onyx marble deposits, NE Turkey. In: *Proceedings of 1st International Symposium on Travertine; Denizli, Turkey*. pp. 171-176.
- Bertini A, Minissale A, Ricci M (2014). Palynological approach in upper Quaternary terrestrial carbonates of Central Italy: anything but a “mission impossible”. *Sedimentology* 61: 200–220. doi: 10.1111/sed.12079
- Bariloro F, Della Porta G, Capezzuoli E (2012). Depositional geometry and fabric types of hydrothermal travertine deposits (Albegna Valley, Tuscany, Italy). *Rendiconti Online Società Geologica Italiana* 21: 1024-1025.
- Beres M, Luetscher M, Oliver R (2001). Integration of ground-penetrating radar and microgravimetric methods to map shallow caves. *Journal of Applied Geophysics* 46 (4): 249-262.
- Braithwaite CJR (1979). Crystal textures of Recent fluvial pisolites and laminated crystalline crusts in Dyfed, South Wales. *Journal of Sedimentary Petrology* 49 (1): 181–193. doi: 10.1306/212F76E9-2B24-11D7-8648000102C1865D
- Capezzuoli E, Gandin A, Pedley M (2014). Decoding tufa and travertine (fresh water carbonates) in the sedimentary record: the state of the art. *Sedimentology* 61: 1-21. doi: 10.1111/sed.12075
- Chafetz HS, Guidry SA (1999). Bacterial shrubs, crystal shrubs, and ray-crystal crusts: Bacterially induced vs abiotic mineral precipitation. *Sedimentary Geology* 126: 57-74. doi: 10.1016/S0037-0738(99)00032-9
- Chafetz HS, Folk RL (1984). Travertines: depositional morphology and the bacterially constructed constituents. *Journal Sedimentary Petrology* 54 (1): 289-316. doi: 10.1306/212F8404-2B24-11D7-8648000102C1865D
- Chafetz HS (2013). Porosity in bacterially induced carbonates: focus on micropores. *AAPG Bulletin* 97 (11): 2103–2111. doi: 10.1306/04231312173
- Cheng H, Edwards RL, Shen CC, Polyak VJ, Asmerom Y et al. (2013). Improvements in ²³⁰Th dating, ²³⁰Th and ²³⁴U half-life values, and U–Th isotopic measurements by multi-collector inductively coupled plasma mass spectrometry. *Earth Planetary Science Letters* 371–372: 82-91. doi: 10.1016/j.epsl.2013.04.006
- Claes H, Erthal MM, Soete J, Özkul M, Swennen R (2017). Shrub and pore type classification: petrography of travertine shrubs from the Ballık-Belevi area (Denizli, SW Turkey). *Quaternary International* 437: 147–163. doi: 10.1016/j.quaint.2016.11.002
- Cook M, Chafetz HS (2017). Sloping fan travertine, Belen, New Mexico, USA. *Sedimentary Geology* 352: 30-44. doi: 10.1016/j.sedgeo.2017.02.010
- Conyers LB (2006). Ground-penetrating radar techniques to discover and map historic graves. *Historical Archaeology* 40: 64–73. doi: 10.1007/BF03376733
- Çapkınoğlu Ş (2003). First records of conodonts from “The Permo-Carboniferous Of Demirözü” (Bayburt), Eastern Pontides, NE Turkey. *Turkish Journal of Earth Sciences* 12: 199-207.
- Della Porta G, Reitner J (2020). The influence of microbial mats on travertine precipitation in active hydrothermal systems (Central Italy). doi: 10.1101/2020.07.29.226266
- De Filippis L, Faccenna C, Billi A, Anzalone E, Brilli M et al. (2012). Growth of fissure ridge travertines from geothermal springs of Denizli Basin, western Turkey. *GSA Bulletin* 124: 1629–1645. doi: 10.1130/B30606.1
- Dokuz A, Aydıncakir E, Kandemir R, Karslı O, Siebel W et al. (2017). Late Jurassic magmatism and stratigraphy in the Eastern Sakarya Zone, Turkey: evidence for the slab breakoff of Paleotethyan oceanic lithosphere. *The Journal of Geology* 125: 1-31. doi: 10.1086/689552
- Erthal MM, Capezzuoli E, Mancini A, Claes H, Soete J et al. (2017). Shrub morpho-types as indicator for the water flow energy-Tivoli travertine case (Central Italy). *Sedimentary Geology* 347: 79-99. doi: 10.1016/j.sedgeo.2016.11.008
- Faccenna C, Soligo M, Billi A, Filippis LD, Funicello R et al. (2008). Late Pleistocene depositional cycles of the Lapis Tiburtinus travertine (Tivoli, central Italy): possible influence of climate and fault activity. *Global and Planetary Change* 63: 299-308. doi: 10.1016/j.gloplacha.2008.06.006
- Folk RL, Chafetz HS (1983). Pisoliths (pisoliths) in Quaternary travertines of Tivoli, Italy. In: Peryt TM (editor). *Coated Grain*. Berlin, Germany: Springer-Verlag, pp. 474-487.
- Fouke BW, Farmer JD, Des Marais DJ, Pratt L, Sturchio NC et al. (2000). Depositional facies and aqueous-solid geochemistry of travertine

- depositing hot springs (Angel Terrace, Mammoth Hot Springs, Yellowstone National Park, U.S.A.). *Journal of Sedimentary Research* 70: 565–585. doi: 10.1306/2dc40929-0e47-11d7-8643000102c1865d
- Gandin A, Capezzuoli E (2008). Travertine versus Calcareous tufa: distinctive petrologic features and stable isotope signatures. *Italian Journal of Quaternary Sciences* 21: 125–136.
- Gandin A, Capezzuoli E (2014). Travertine: distinctive depositional fabrics of carbonates from thermal spring systems. *Sedimentology* 61: 264–290. doi: 10.1111/sed.12087
- Guo L (1993). Fabrics and facies of Quaternary travertines, Rapolano Terme, central Italy. PhD, University of Wales, Cardiff, UK.
- Guo L, Riding R (1998). Hot-spring travertine facies and sequences, Late Pleistocene Rapolano Terme, Italy. *Sedimentology* 45: 163–180. doi: 10.1046/j.1365-3091.1998.00141.x
- Güven İH (1993). Doğu Pontidlerin 1/250.000 ölçekli komplikasyonu, Maden Tetkik Arama Genel Müdürlüğü, Ankara.
- Hancock PL, Chalmers RML, Altunel E, Çakır Z (1999). Travertines: using travertines in active fault studies. *Journal of Structural Geology* 21: 903–916. doi: 10.1016/S0191-8141(99)00061-9
- Hiess J, Condon DJ, McLean N, Noble SR (2012). $^{238}\text{U}/^{235}\text{U}$ systematics in terrestrial uranium-bearing minerals. *Science* 335: 1610–1614. doi: 10.1126/science.1215507
- Jaffey AH, Flynn KF, Glendenin LE, Bentley WC, Essling AM (1971). Precision measurement of half-lives and specific activities of ^{235}U and ^{238}U . *Physical Review C* 4: 1889–1906.
- Jones FG, Wilkinson BH (1978). Structure and growth of lacustrine pisoliths from recent Michigan marl lakes. *Journal of Sedimentary Petrology* 48: 1103–1111.
- Jones B, Renaut RW (2008). Cyclic development of large, complex calcite dendrite crystals in the Clinton travertine, Interior British Columbia, Canada. *Sedimentary Geology* 203: 17–35. doi: 10.1016/j.sedgeo.2007.10.002
- Jones B, Renaut RW (2010). Calcareous spring deposits in continental settings. In: *Carbonates in Continental Settings: Facies, Environments, and Processes* (Eds A.M. Alonso Zarza and L.H. Taner), *Development in Sedimentology* 61: 177–204.
- Kadioğlu S (2008). Photographing layer thicknesses and discontinuities in a marble quarry with 3D GPR visualization. *Journal of Applied Geophysics* 64 (3-4): 109–114. doi: 10.1016/j.jappgeo.2008.01.001
- Kandemir R (2004). Sedimentary characteristics and depositional conditions of Lower-Middle Jurassic Şenköy Formation in and around Gümüşhane. PhD, Karadeniz Technical University, Trabzon, Turkey (in Turkish).
- Karaisaloğlu S, Orhan H (2018). Sedimentology and geochemistry of the Kavakköy Travertine (Konya, central Turkey). *Carbonates and Evaporites* 33: 783–800. doi: 10.1007/s13146-018-0436-z
- Karsli O, Dokuz A, Kandemir R (2016). Subduction-related Late Carboniferous to Early Permian Magmatism in the Eastern Pontides, the Camlik and Casurluk plutons: Insights from geochemistry, whole-rock Sr–Nd and in situ zircon Lu–Hf isotopes, and U–Pb geochronology. *Lithos* 266–257: 98–114. doi: 10.1016/j.lithos.2016.10.007
- Kele S, Özkul M, Gökgöz A, Fözis I, Baykara MO et al. (2011). Stable isotope geochemical and facies study of Pamukkale travertines: new evidences of low-temperature non-equilibrium calcite-water fractionation. *Sedimentary Geology* 238: 191–212. doi: 10.1016/j.sedgeo.2011.04.015
- Mancini A, Frondini F, Capezzuoli E, Galvez Mejia E, Lezzi G et al. (2019). Porosity, bulk density and CaCO_3 content of travertines. A new dataset from Rapolano, Canino and Tivoli travertines (Italy). *Journal of Data in Brief* 25:104158. doi: 10.1016/j.dib.2019.104158
- Mendonça-Filho JG, Menezes TR, Oliveira-Mendonça J, Donizeti de Oliveira A, Freitas da Silva T et al. (2012). *Organic Facies: Palynofacies and Organic Geochemistry Approaches, Geochemistry - Earth's System Processes*, Dr. Dionisios Panagiotaras (Ed.), ISBN: 978-953-51-0586-2, InTech, Available from: <http://www.intechopen.com/books/geochemistry-earth-s-system-processes/organic-facies-palynofacies-andorganic-geochemistry-approaches>
- Minissale A, Kerrick DM, Magro G, Murrell MT, Paladini M et al. (2002). Geochemistry of Quaternary travertines in the region north of Rome (Italy): structural, hydrologic and paleoclimatologic implications. *Earth and Planetary Science Letters* 203: 709–728. doi: 10.1016/S0012-821X(02)00875-0
- Minissale A, Sturchio NC (2004). Travertines of Tuscany and Latium (Central Italy) Florence. In: *International School of Travertine and Tufa; Abbadia San Salvatore, Italy*. P25.
- Okay AI, Leven EJ (1996). Stratigraphy and paleontology of the Upper Paleozoic sequence in the Pulur (Bayburt) region, Eastern Pontides. *Turkish Journal of Earth Sciences* 5: 145–155.
- Okay AI, Şahintürk Ö (1997). Geology of the Eastern Pontides. In: Robinson AG (editor). *Regional and petroleum geology of the Black Sea and surrounding region. USA, American Association of Petroleum Geologists Memoir* 68: pp. 291–311.
- Okay AI, Tüysüz O (1999). Tethyan sutures of northern Turkey. In: Durand B, Jolivet L, Horváth F, Séranne M (editors). *The Mediterranean Basins: Tertiary Extension within the Alpine Orogen. Geological Society of London Special Publications* 156: 475–515.
- Öğretmen Z, Şeren A (2014). Investigating fracture-crack systems with geophysical methods in Bayburt Kiratlı travertine. *Journal of Geophysics and Engineering* 11 (6): 065009. doi: 10.1088/1742-2132/11/6/065009
- Özkul M, Varol B, Alçiçek MC (2002). Depositional environments and petrography of Denizli travertines. *Bulletin of the Mineral Research and Exploration* 125: 13–29.
- Özkul M, Kele S, Gökgöz A, Shen CC, Jones B et al. (2013). Comparison of the Quaternary travertine sites in the Denizli extensional basin based on their depositional and geochemical data. *Sedimentary Geology* 294: 179–204. doi: 10.1016/j.sedgeo.2013.05.018
- Özyurt M, Kırmacı MZ, Al-Aasm IS (2019). Geochemical characteristics of Upper Jurassic – Lower Cretaceous platform carbonates in Hazine Mağara, Gümüşhane (northeast Turkey): implications for dolomitization and recrystallization. *Canadian Journal of Earth Sciences*, 56 (3): 306–320. doi:10.1139/cjes-2018-0168
- Pedley HM (2009). Tufas and travertines of the Mediterranean region: a testing ground for freshwater carbonate concepts and developments. *Sedimentology* 56: 221–246. doi: 10.1111/j.1365-3091.2008.01012.x
- Pentecost A (2005) *Travertine*. Berlin, Germany: Springer.
- Pelin S (1977). Alucra (Giresun) Güneydoğu Yöresinin petrol olanakları bakımından jeolojik incelenmesi. *Karadeniz Teknik Üniversitesi Yer Bilimleri Dergisi* 13: 38–42 (in Turkish).
- Porsani LJ, Sauck WA, Junior AOS (2006). GPR for Mapping fractures and as a guide for extraction of ornamental granite from a quarry: a case study from southern Brazil. *Journal of Applied Geophysics* 58: 177–87. doi: 10.1016/j.jappgeo.2005.05.010
- Rainey DK, Jones B (2005). Radiating calcite dendrites- precursors for coated grain formation in the Fairmont Hot Springs Travertine, Canada. In: *Proceedings of International Symposium on Travertine, Denizli, Turkey*. pp. 21–25.
- Ricketts JW, Ma L, Wagler AE, Garcia VH (2019). Global travertine deposition modulated by oscillations in climate. *Journal of Quaternary Science* 34: 558–568. doi: 10.1002/jqs.3144.

- Shäfer A, Stapf KRG (1978). Permian Saar-Nahe Basin and Recent Lake Constance (Germany): two environments of lacustrine algal carbonates. In: Matter A, Tucker ME (editors). *Modern and Ancient Lake Sediments*. The International Association of Sedimentologists Oxford, UK: Wiley, pp. 83–107.
- Shen C-C, Wu C-C, Cheng H, Edwards RL, Hsieh Y-T et al. (2012). High-precision and high-resolution carbonate ^{230}Th dating by MC-ICP-MS with SEM protocols. *Geochimica et Cosmochimica Acta* 99: 71-86. doi: 10.1016/j.gca.2012.09.018
- Silva CCN, Medeiros WE, Sá EFJ, Neto PX (2004). Resistivity and ground-penetrating radar images of fractures in a crystalline aquifer: a case study in CaiÇara farm-NE Brazil. *Journal of Applied Geophysics* 56: 295–307. doi: 10.1016/j.jappgeo.2004.08.001
- Şaffak D (2018). Bahçecik (Tekke-Gümüşhane) travertenlerinin sedimentolojik, paleoklimsel ve yer radarı (GPR) verilerinin incelenmesi. Yüksek Lisans, Recep Tayyip Erdoğan University, Rize, Turkey (in Turkish).
- Tagliasacchi E, Kayseri-Özer MS (2020). Multidisciplinary approach signals of the non-marine carbonates: the case of the Sarıkavak tufa deposits (Afyon, SW-Turkey). *Quaternary International* 544: 41-56. doi: 10.1016/j.quaint.2019.12.016
- Teboul PA, Durllet C, Gaucher EC, Virgone A, Girard JP et al. (2016). Origins of elements building travertine and tufa: new perspectives provided by isotopic and geochemical tracers. *Sedimentary Geology* 334: 97–114. doi: 10.1016/j.sedgeo.2016.01.004
- Tokel S (1972). Stratigraphical and Volcanic History of the Gümüşhane Region, PhD, University College of London, England.
- Toker E, Kayseri-Özer MS, Özkul M, Kele S (2015). Depositional system and palaeoclimatic interpretations of Middle to Late Pleistocene travertines: Kocabaş, Denizli, SW Turkey. *Sedimentology* 62 (5): 1360-1383. doi: 10.1111/sed.12186
- Toker E (2017). Quaternary fluvials tufas of Sarıkavak area, southwestern Turkey: Facies and depositional systems. *Quaternary International* 437 (Part A): 37-50. doi: 10.1016/j.quaint.2016.06.034
- Topuz G, Altherr R, Schwarz WH, Dokuz A, Meyer HP (2007). Variscan amphibolite-facies rocks from the Kurtoğlu metamorphic complex, Gümüşhane area, Eastern Pontides, Turkey. *International Journal of Earth Sciences* 96:861-873. doi: 10.1007/s00531-006-0138-y
- Turhan E (2007). Denizli yöresi (Batı Anadolu) traverten tipi karbonatların fasiyes özellikleri. Master's thesis, İzmir, Turkey (in Turkish).
- Wright VP (2012). Lacustrine carbonates in rift settings: the interaction of volcanic and microbial processes on carbonate deposition. *Geological Society of London, Special Publication* 370: 39–47. doi: 10.1144/SP370.2
- Yalçınır CÇ (2013). Investigation of subsurface geometry of fissure-ridge travertine with GPR, Pamukkale, western Turkey. *Journal of Geophysics and Engineering* 10 (3): 035001. doi: 10.1088/1742-2132/10/3/035001
- Yalçınalp B, Ersoy H, Fırat Ersoy A, Keke C (2008). Bahçecik (Gümüşhane) Travertenlerinin Jeolojik ve Jeoteknik Özellikleri. *Jeoloji Mühendisliği Dergisi* 32: 25-39.
- Yılmaz C, Kandemir R (2006). Sedimentary records of the extensional tectonic regime with temporal cessation: Gümüşhane Mesozoic Basin (NE Turkey). *Geologica Carpathica* 57 (1): 3–13.
- Yılmaz C, Carranante G, Kandemir R (2008). The rift-related Late Cretaceous drowning of the Gümüşhane carbonate platform (NE Turkey). *Bollettino Societa Geologica Italiana* 127 (1): 37-50.
- Yoshimura K, Liu Z, Cao J, Yuan D, Inokura Y et al. (2004). Deep source CO₂ in natural waters and its role in extensive tufa deposition in the Huanglong Ravines, Sichuan, China. *Chemical Geology* 205: 141–153. doi: 10.1016/j.chemgeo.2004.01.004